*International Journal of Latest Engineering and Management Research (IJLEMR)*
*ISSN: 2455-4847*
*www.ijlemr.com || Volume 08 – Issue 03 || March 2023 || PP. 117-131*

# Characterization of Acalypha Wilkesiana Leaf Extract by FT-IR and GC–MS as Green Inhibitor for Ferritic Stainless Steel in 1 M Nacl

[1]Elenwo, O.P. and [2]Uchegbulam, I.
*[1]Department of Physics, Faculty of Science University of Port Harcourt, P.M.B.5323, Choba, Rivers State Nigeria.*
*[2]Department of Production Technology;*
*School of Science Laboratory Technology, University of Port Harcourt, P.M.B.5323*

**Abstract:** The study examined the possibility of characterizing extract ofAcalypha wilkesiana (AW)leaf as green inhibitor for ferritic stainless steel (FSS) by FT-IR and GC-MS in 1M Nacl. This was obtained using gravitational weight loss, Potentiodynamic polarization techniques, Scanning electron microscopy (SEM), Electrochemical Impedance Spectroscopy (EIS). The inhibitor, temperature and time concentration ranged from 0–10 percent v/v at 2 percent v/v interval to 30–60 ° C at 10 ° C interval at 3-18 days within a space of three days. Qualitative and quantitative analysis, Gas Chromatography-Mass Spectrometry (GC-MS), Fourier Transforms Infrared (FTIR) Spectroscopy techniques were used to characterize the sample. Scanning Electron Microscope (SEM) was used to analyze the sample surface morphology before, during and after testing. The findings showed that the corrosion rate increased with a rise in temperature and decreased with a rise in inhibitor concentration Inhibition effectiveness of 93.17%-93.60% was obtained as the immersion time increases from 9 days to 18 days in 1M Nacl. There was an enhancement with a soft green inhibitor on the surface morphology of ferritic stainless steel. The adsorption and physisorption in nature of the extract obeys Langmuir adsorption isotherm. The inhibition effectiveness values acquired are well above a good inhibitor's minimum acceptable threshold of 70 percent. Therefore, the Acalypha Wilkesiana (AW) extract was very efficient in inhibiting FSS corrosion in alkaline medium.

**Keywords:** Characterization, Acalypha-Wilkesiana, FT-IR, GC–MS, Ferritic Steel.

## Introduction

Structural materials are handled to alter their surface characteristics for decoration, enhanced hardness, wear resistance, corrosion mitigation or a basis for improving adherence to other treatments such as painting or photosensitive printing coatings (STMP, 2006). In both natural and industrial settings, these materials are volatile and inevitably return to stable chemical species similar to the chemically mixed forms from which they were obtained (Khadroui, et al; 2016). Most of the synthetic compounds used as corrosion inhibitors, although in most cases have excellent anti-corrosion characteristics, are extremely toxic to humans and the environment. Synthetic chemicalbased inhibitors may cause temporary or permanent harm to human organs or interfere with human biochemical procedures. The toxicity may occur during the synthesis of the compound (Suleiman, et al; 2017). The development of novel and non-toxic corrosion inhibitors from certain components of low-cost natural substances has been considered as financial, strategic and environmentally plausible advantage. A basic field of research is the discovery of plant products as environmentally friendly inhibitors of corrosion. In plant products, the electronic and molecular structures are similar to those of the usual inhibitor molecules (Rekkab, et al; 2012 and Dourna, et al; 2011). Acalypha wilkesiana is a plant belonging to the Euphorbiacaece family. The genus Acalypha crops are discovered all over the globe, particularly in the tropics of Africa, America, Asia, and from other areas of the globe have been brought into West Africa. It was grown in gardens and greenhouses as leaf crops (Petchiamal, et al; 2013). It gives a bronze red to muted red splash of color in the landscape, the leaves appear as heart-shaped. Acalyphawilkesiana has been reported to be used in hypertension therapy, particularly in the management of abnormal sodium and potassium metabolism accompanying hypertension (Rajendran and Karthikeyan , 2012). Figure 1 shows the picture of Acalypha wilkesiana (AW) leaf.

Figure 1: Acalypha wilkesiana(AW) copper leaf or Joseph's coat leaf

## Materials and Methods

**Preparation of the stainless steel**

The material used for the study is ferritic stainless steel of rectangular shape with lengths of 12.5 mm, width of 6.5 mm, and thickness of 1.5 mm. The ferritic stainless steel was sourced from Mudiame International Limited Port-Harcourt, Nigeria. The chemical composition test as showed in Table1 was carried out at the Department of Metallurgical and Materials Engineering Laboratory, Federal University of Technology, Owerri, Imo State. The chemical analysis was carried out using spark analysis.

**Sample preparation for the experiment**

To conduct the weight loss experiment the metals were cut into 12.5 mm by 6.5 mm sizes. They were then subjected to chemical treatments. The ferritic steel samples were subjected to chemical treatments such as degreasing before immersing in benzene and then dried. It was then immersed in a solution of HCl with acid to water ratio of 1 to 8 for 2 0 minutes at room temperature. They were then dried with clean cloth and stored in a desiccator.

Table1: Elemental composition of ferritic stainless steel deployed for the study

| S. No. | Metal | (Wt. %) Elemental Composition |
|---|---|---|
| 1 | Fe | Balance |
| 2 | C | 0.0880 |
| 3 | Si | 0.471 |
| 4 | Mn | 9.230 |
| 5 | P | 0.112 |
| 6 | S | 0.0294 |
| 7 | Cr | 17.42 |
| 8 | Ni | 1.15 |
| 9 | Mo | <0.001 |
| 10 | Cu | 0.791 |
| 11 | Al | 0.0061 |
| 12 | Ti | 0.0137 |
| 13 | V | 0.0968 |
| 14 | Co | 0.129 |
| 15 | Nb | 0.029 |
| 16 | Sn | 0.0195 |
| 17 | Pb | 0.0208 |
| 18 | Mg | 0.0103 |
| 19 | As | 0.0887 |
| 20 | Ce | 0.0111 |
| 21 | Ta | 0.150 |
| 22 | Zn | 0.273 |
| 23 | N | 0.0414 |

**Solution Preparation**

Solutions of 1M Nacl were set up in order to dilute systematic grade with twofold refined (distilled) water. Concentrate was dissolved in the acid solution at the required concentration (% v/v). The solution without inhibitor was taken as clear for correlation purposes. The test solutions were newly arranged before each trial by adding Acalypha wilkesiana straight to the acid solution. Concentration of Acalypha wilkesiana extract0, 2, 4, 6, 8, and 10 % v/v. Examinations/tests were performed in triplicate to guarantee great outcomes as shown in Table 2

Table 2 : Experimental design for the corrosion tests

| Solutions | Compositions of the Media/extract |
|---|---|
| $A^0$ | 1M NaCl solution |
| A1 | Sodium benzoate (SB) + 1M NaCl solution (SB: 2, 4, 6, 8, and 10% v/v) and the concentration of 1M NaCl solution remained constant. |
| A2 | Acalypha wilkesiana (AW) + 1M NaCl solution (AW: 2, 4, 6, 8, and 10% v/v) and the concentration of 1M NaCl solution remained constant. |

**Inhibitor Preparation**

Acalypha wilkesiana(AW) used was obtained from the university of Port-Harcourt, Rivers State in Nigeria. The AW was extracted in 1.5 litres of 70% ethanol and 30% distilled water as solvent and half the AW was extracted using maceration method. The ethanol was evaporated by using a water bath and the concentration of the stock solution expressed in terms of (% v/v) and the concentration of2–10% v/v of the extract as prepared according to (Adindu and Oguzie, 2017 and Kubmarawa, et al; 2007).

**Characterization of Acalypha wilkesiana (AW) by phytochemical and FTIR analyses**

The phytochemical constituents were carried out by qualitative/quantitative methods at National Research Institute of Chemical Technology, Zaria. The qualitative and quantitative results showed that the Acalypha wilkesiana (AW) leaf contains Saponins, Tannins, Alkaloids, Flavonoids, Glycosides and Volatile oil. Fourier Transforms Infrared (FTIR) analysis was carried out to determine the functional groups and chemical bonds. It was carried out using -8400S spectrophotometer Schmadzu Product Japan at National Research Institute Chemical Technology Zaria. The spectra recorded and the interpretations were done by using Standard Library. Both the phytochemical analyses and FTIR were presented in tables 3 and 4 respectively.

**Methods used for corrosion techniques**

Previously polished and degreased stored coupons were used for weight loss studies. Specimens that have been weighed differently soaked in 500 mL of 1 M Nacl solutions containing 0, 2, 4, 6, 8 and 10% v/v of AW extract for 3, 6, 9, 12, 15, and 18days. After sometime, when it was time, the specimens were taken out, washed, dried and reweighed. The staged up experiments were carried out thrice while at the same time their mean values were put down. This experiment was repeated 4 times with varying temperatures of 30, 40, 50, and 60°C, respectively. From the deliberate weight reduction information, the corrosion rate (mpy) and the restraint productivity (inhibition efficiency) (IE) were determined utilizing equipments 1 - 3 (Adindu and Oguzie, 2017). The corrosion rate (CR) of the material loss as a result of chemical reaction can be expressed as the thickness loss of the stainless steel per unit time:

$$CR = \frac{534W}{DAT} \quad (1)$$

Where W is the weight loss after exposure of time t, D and A are the density and exposed area while the 534 is a constant respectively. CR in mils per year (mpy) and W, D, A and t will be in units of milligrams, grams per cubic centimeter ($g/cm^3$), square inches and hours.

$$\left(\frac{CR_a}{CR_p}\right) x\ 100 \quad (2)$$

$$\theta = \frac{CR_a - CR_p}{CR_a} \quad (3)$$

Where $CR_a$, $CR_p$ and θ are corrosion rates in the absence, presence and degree of surface coverage of the inhibitor respectively.

**Potentiodynamic Polarization (Tafel plots)**

All test have been completed in open circuit potential (OCP-T) under barometrical conditions at a temperature of 30°C utilizing three-cathode frameworks including a calomel reference terminal, a platinum plate as the helper anode and ferritic stainless steel tests as working anode that drenched in 1 M Nacl solutions. In Tafel test, after a deferral of around 15 minutes, the potential was expanded with 1 mV/s filtering rate. The required information were gotten utilizing the above programming. From the exploratory estimations, the estimations of corrosion potential (Ecorr), corrosion current thickness (Icorr) anodic and cathodic Tafel slope constants (ba and bc) can be assessed from the anodic and cathodic points of Tafel plots. However, the extrapolation of the linear Tafel portion of the anodic and cathodic plot to corrosion potential was done to obtain corrosion current densities (Icorr). The inhibition efficiency (IE %) of the inhibitor was calculated using equation 4 (Adindu and Oguzie, 2017):

$$IE\ \% = \frac{i_{corr} - i'_{corr}}{i_{corr}} x\ 100\% \quad (4)$$

Where $i_{corr}$ and $i'_{corr}$ are the rust current densities of ferritic stainless steel in the absence and presence of the inhibitor respectively as described (Suleiman and Abdulwahab, 2016).

**SEM investigations**

The stainless-steel surface was prepared for SEM by keeping the specimens for one hour in the electrolyte, with and without the ideal fixations of the inhibitor. The treated steel examples were then washed with refined water, dried and broken down utilizing SEM. A Philips model XL30SFEG examining electron microscope was utilized for surface examination. The stainless-steel surface, as described by Suleiman et al; (2018).

**Electrochemical Impedance Spectroscope**

The impedance measurement technique was applied to study the pitting corrosion and other localized corrosion (Hamdy et al, 2006). The impedance technique has advantages in the study of interfacial reactions and other interfacial phenomena. The impedance information obtained also has time resolved and surface-averaged characteristics (Zhang et al, 1993).

In this work, the corrosion behaviour of ferritic stainless-steel specimens was investigated using electrochemical impedance spectroscopy (EIS) in 1M NaCl. Nyquist plot in figures 6 showed that the corrosion resistance increased with increasing extract concentrations. The Nyquist plots at high frequencies, yielded an impedance loop with high charge transfer resistance in the presence AW extract and very small charge transfer resistance in the absence of the extract. The various charge transfer resistances, represents an inhibitor environment with large corrosion resistance, and an inhibitor free environment with very little corrosion resistance. The EIS results indicate that the Rct values increased with increasing additive concentration. The percentage of inhibition efficiency (IE %) was calculated from the charge transfer resistance (Rct) values. The efficiency increased with increase in concentration of the extract with a maximum efficiency of 95% at 8%v|v concentration of the extract. These results confirm the important role of AW to enhance the formation of protective oxide films that shifted the current to more noble one and consequently, reducing the number of pits. Therefore, it can be assumed that a layer of the inhibitor was formed at the metal/solution interface, thus improving corrosion inhibition (Gerengi et al; 2009; Popova and Christov, 2006). It can therefore, be attributed to the fact that adsorption of phytoconstituents obtained from both FT-IR and GC-MS spectroscopy (functional groups, aromatic hydrocarbons compounds and molecular structures) resulted in the formation of a protective layer. Thus decreased the electron transfer between the metal surface and the corrosive medium (Chetouani et al., 2004; Saratha and Vasudha, 2009). According to the Bode plots presented in figure 7 there were dramatic decrease of the impedance in the capacitive region, which is a characteristic of the pitting process on stainless

steel. In addition, the phase angle tended toward zero at low frequencies in fig.8, indicating that the resistance of the barrier layer was being approached.

## Results and Discussions

**Chemical Composition of ferritic stainless steel**

Table 1 showed the chemical composition of the as-received ferritic stainless steel which was determined by spark analysis at Federal University of Technology, Owerri, Nigeria.

**Characterization of Acalypha wilkesiana (AW)**

**The experimental design for the corrosion tests was shown in Table 2**

**Phytochemical analyses**

The Quantitative and qualitative phytochemical screenings of the leaf extract (Acalypha wilkesiana, AW) in percentage (%) and mg/100mg results are presented in Tables 3 and 4. The results also indicated that the leaf extract contains tannins, alkaloids, flavonoids, saponins, glycosides and volatile oil.

Table 3: Quantitative analysis of Acalypha wilkesiana (AW) leaf

| S/No | Leaf | Alkaloids (%) | Tannins (mg/100 g) | Saponins (%) | Flavonoids (%) | Glycosides (mg/100 g) | Volatile oil (%) |
|---|---|---|---|---|---|---|---|
| 1 | AW | 10.04 | 1281 | 6.98 | 6.32 | 870 | 3.03 |

Table 4: Qualitative analysis of Acalypha wilkesiana (AW) leaf

| S/No | Leaf | Alkaloids | Tannins | Saponins | Flavonoids | Glycosides | Volatile oil |
|---|---|---|---|---|---|---|---|
| 1 | AW | ++ | +++ | ++ | + | +++ | + |

Heavily present: +++; slightly present: ++; present: +; absent: −

Fourier Transforms Infrared (FTIR) Spectroscopic method Table 5 showed the peaks and intensity while table 6 showed the outstanding peak obtained from reflectance for AW extract reflectance FT-IR spectroscopy. The IR absorption bands between 524.66 to 3402.54 $cm^{-1}$ for Acalypha wilkesiana indicated the presence of Suphides compound (SxOy compounds, P=O vibration for stretching vibrator organic phosphorustion, $CH_2$, R-CH = CH-R, C=$CH_2$ mono, 1,1, C=C stretch, -N=C=S, C=N, $CH_2$, $NH_2$, X=Y and X=Y=Z, $NH_2$ functional groups which fit well with these constituents. Figures 2 and 3 presented the results of chemical bonds/functional groups of IR absorption spectrum of AW extract from the tables.

Table 5: Peaks and intensity for AW extract from reflectance FT-IR spectroscopy

| No. | Peak | Intensity | Corr. Intensity | Base (H) | Base (L) | Area | Corr. Area |
|---|---|---|---|---|---|---|---|
| 1 | 524.66 | 72.158 | 1.261 | 547.8 | 486.08 | 8.439 | 0.239 |
| 2 | 609.53 | 68.801 | 4.029 | 640.39 | 563.23 | 11.624 | 1.021 |
| 3 | 663.53 | 71.006 | 3.654 | 848.71 | 640.39 | 20.266 | 1.391 |
| 4 | 902.72 | 86.953 | 0.878 | 918.15 | 848.71 | 3.77 | 0.198 |
| 5 | 1041.6 | 60.157 | 7.059 | 1072.46 | 918.15 | 23.783 | 3.248 |
| 6 | 1149.61 | 55.623 | 11.653 | 1280.78 | 1072.46 | 42.042 | 8.074 |
| 7 | 1334.78 | 65.883 | 3.955 | 1357.93 | 1280.78 | 12.377 | 1.095 |
| 8 | 1381.08 | 67.031 | 2.511 | 1489.1 | 1357.93 | 19.126 | 1.511 |
| 9 | 1635.69 | 49.735 | 38.148 | 1851.72 | 1489.1 | 49.14 | 31.158 |
| 10 | 2353.23 | 65.141 | 22.624 | 2399.53 | 1867.16 | 26.252 | 8.966 |
| 11 | 2870.17 | 63.372 | 0.443 | 2877.89 | 2399.53 | 55.43 | -6.714 |
| 12 | 2931.9 | 56.587 | 4.666 | 2985.91 | 2877.89 | 24.764 | 1.739 |
| 13 | 3402.54 | 23.246 | 1.136 | 3734.31 | 3394.83 | 130.488 | -1.385 |

Table 6: Prominent peaks obtained from reflectance FTIR spectroscopy for AW extra

| No. | Frequency ($cm^{-1}$) | Band assignment |
|---|---|---|
| 1 | 524.66 | Metal –O- metal group |
| 2 | 609.53 | C-I Stretching of iodol compound |
| 3 | 663.53 | C-Br Stretching of halogen derivatives |
| 4 | 902.72 | Thiocarbonyl (C=S) |
| 5 | 1041.6 | Sulphides compound (SxOy compounds) |
| 6 | 1149.61 | Symmetric stretching of amino acids |
| 7 | 1334.78 | P=O Vibration for stretching vibrator organic phosphorustion |
| 8 | 1381.08 | $C(CH_3)_3$ |
| 9 | 1635.69 | N-H in =plane bending mainly proteins |
| 10 | 2353.23 | PH acids) stretches (Phosphoric |
| 11 | 2870.17 | $CH_2$ Symmetric stretching of amino acids |
| 12 | 2931.9 | C-H stretching mainly lipids |
| 13 | 3402.54 | N-H stretching amine |

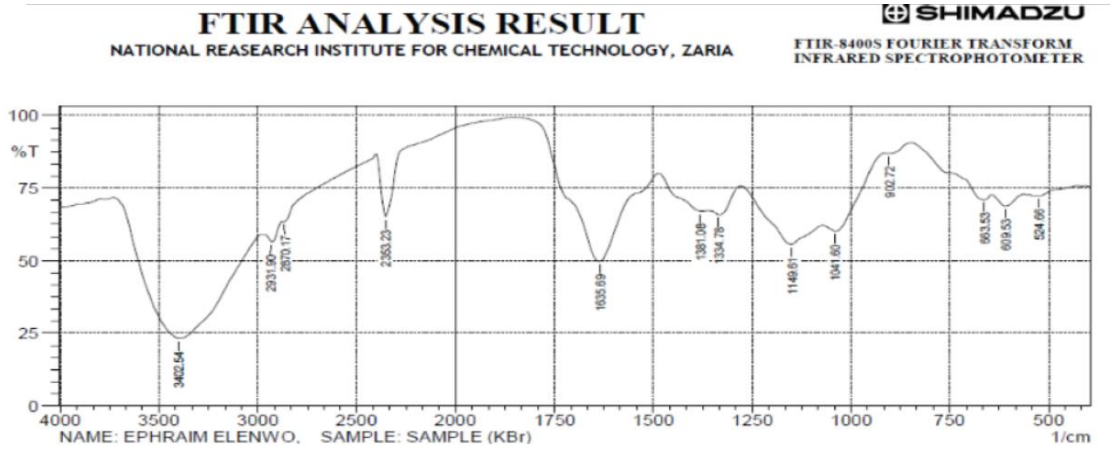


Figure 2: IR absorption spectrum of AW bark extract

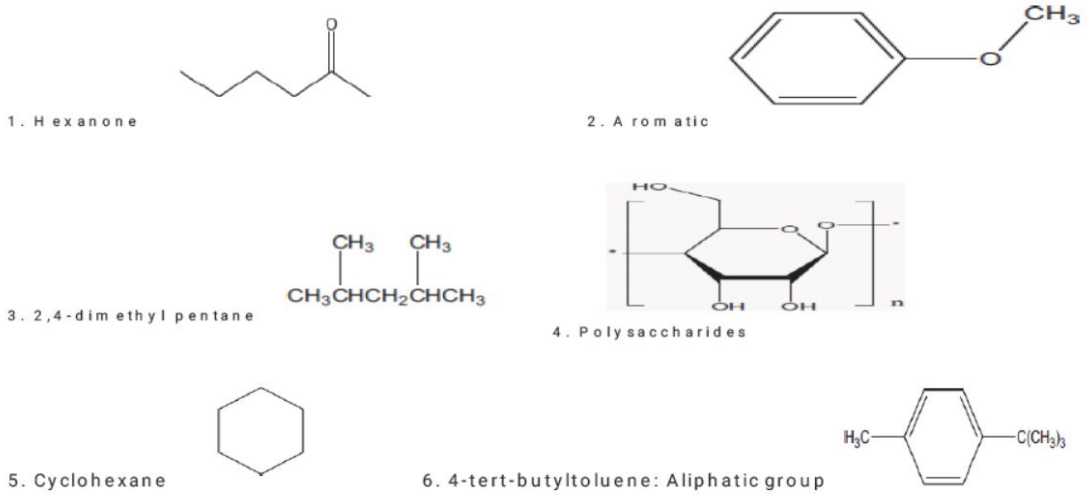


Figure 3: Chemical bonds/Functional groups of IR Absorption Spectrum of AWExtract.

Weight loss (WL) measurements The corrosion rate was displayed on Figure 4, as well as the time for the corrosion of ferritic stainless steel (FSS) in 1 M Nacl containing various concentrations of AW at 40°C. From the figure, it is evident that the corrosion rate of ferritic stainless-steel decreases with increase in the concentration of AW. The corrosion rate of the FSS in the absence of the inhibitor (blank) solution was higher than those obtained for solutions of Nacl containing various concentrations of AW. The decline in the corrosion rates can be ascribed to a portion of the constituents that were contained in the extract such as functional groups, hydroxyl, aromatic / heterocyclic rings compounds present and the metallic elements that reacted with some cations to form protective films on the samples. Table 7 analysis on the optimum concentration for Acalypha wilkesiana (AW) was 8% v/v with utmost reticence competence (inhibition efficiency) of 90.50% for the period of 18 days of immersion time. This result indicated that the plant extract could act as effective corrosion inhibitor for FSS in the sodium chloride medium. This indicated that the reaction of the inhibitor on the surface of the FSS has reached the state of equilibrium.

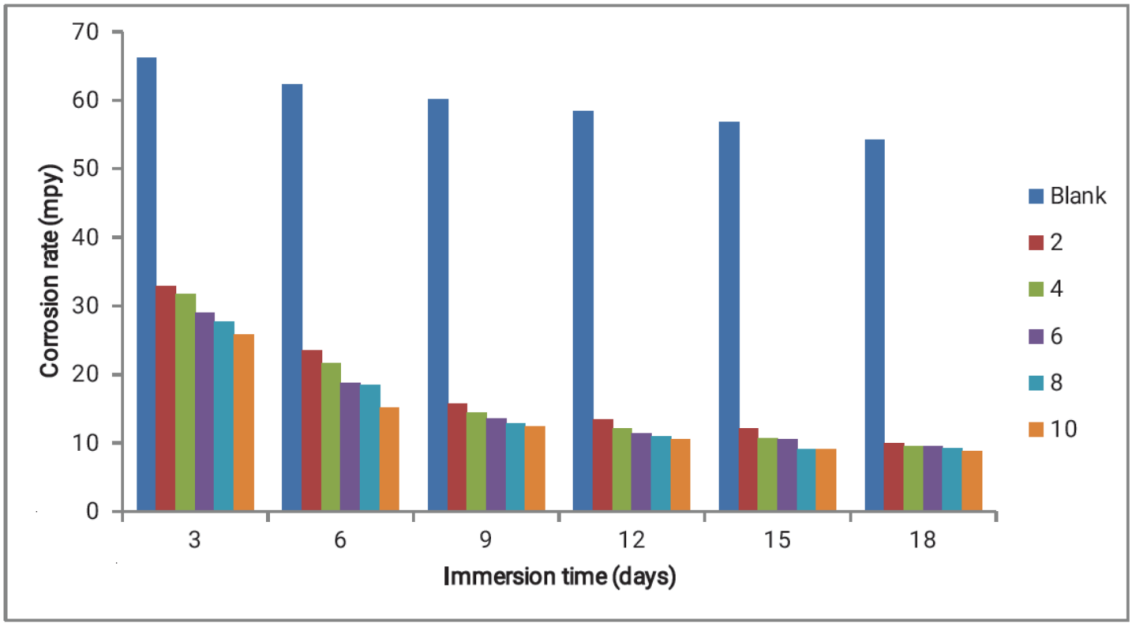


Figure 4: Variation of Corrosion Rate with immersion time of AW extract for stainless steel in 1M NaCl solution at 40ºC

Table 7: Inhibition efficiencies (%) of FSS in absence and presence of AW in 1M NaCl at at40°C

| Conc.(% v/v) | Inhibition efficiency (IE %) | | | | | |
|---|---|---|---|---|---|---|
| Time (Days) | 3 | 6 | 9 | 12 | 15 | 18 |
| Blank | - | - | - | - | - | - |
| 2 | 79.70 | 80.00 | 80.90 | 81.30 | 81.30 | 81.80 |
| 4 | 80.90 | 82.00 | 82.20 | 84.00 | 84.60 | 84.90 |
| 6 | 83.40 | 83.70 | 84.40 | 85.80 | 85.90 | 86.10 |
| 8 | 84.90 | 85.20 | 86.90 | 88.90 | 89.10 | 90.30 |
| 10 | 86.70 | 87.60 | 89.20 | 89.80 | 89.80 | 90.50 |

Potentiodynamic polarization The results presented in Figure 5 demonstrated the impact of AW extract on both cathodic and anodic polarization curve of ferritic tempered steel in 1M Nacl. It could be seen that both the cathodic and anodic responses were stifled with the expansion of explored green inhibitor extricate, which proposed that AW concentrate decreased anodic disintegration and furthermore hindered the hydrogen advancement response. Electrochemical corrosion energy parameters, for example corrosion potential (Ecorr), cathodic and anodic Tafel slants (βa, βc) and corrosion current thickness ($i_{corr}$) got from the extrapolation of the polarization bends, were additionally given in table 8 were calculated using equation 4. The values given in the tables show that, corrosion current (icorr) decreases noticeably in the occurrence of the extract. The magnitudes of change increase with increasing extract inhibitor concentrations. This confirms the inhibitive action of the AW on ferritic stainless steel in sodium chloride. The current densities decrease with increase in the extract concentrations from 2-10% v/v, which suggests that passive layer on the surface of ferritic stainless steel is

strengthened in the presence of extract due to blockage of active sites on the electrode surface and agreed to (Ahmed et al;2014 and Anupama, et al;2016). This decrease in $i_{corr}$ was related to the adsorption of the inhibitor on ferritic stainless steel/acid solution interface and confirmed to the previous works (Suleiman and Abudlwahab, 2016).

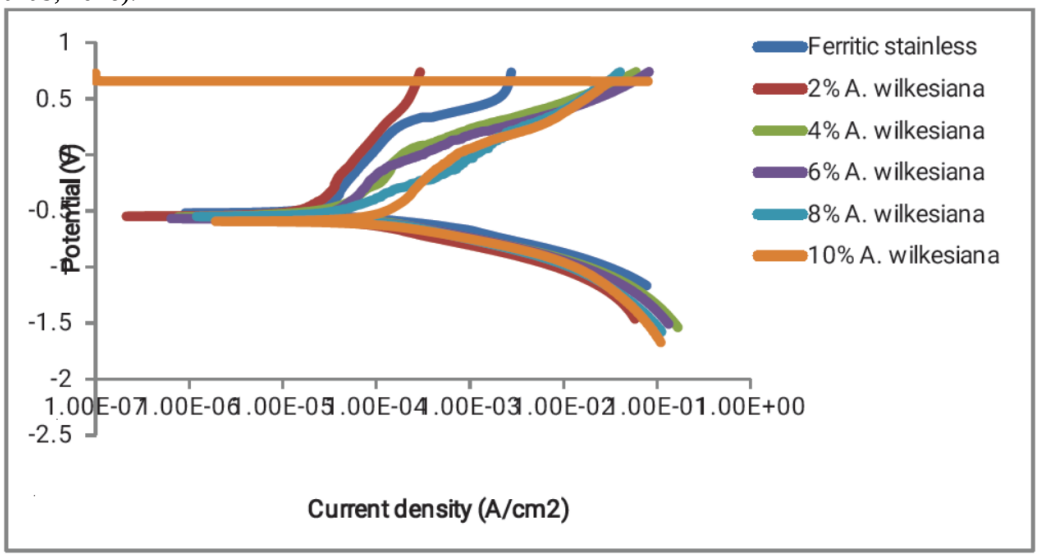


Figure 5: Potentiodynamic polarization curves of ferritic stainless steel in 1M NaCl solution in the absence and presence of Acalypha wilkesiana (AW) concentrations at 30°C

Table 8: Potentiodynamic polarization parameters for ferritic stainless steel in 1M NaCl containing different concentrations of AW extract at 30°C

| AW (% v/v) | -Ecorr (SCE) (mV) | Iorr (mA/cm$^2$) | Tafel slopes (mV/decade) | | Inhibition efficiency |
|---|---|---|---|---|---|
| | | | $b_a$ | $b_c$ | |
| Control | 0.524 | 7.88 | 79 | 84 | - |
| 2 | 0.548 | 1.91 | 91 | 84 | 75.76 |
| 4 | 0.589 | 1.42 | 93 | 85 | 81.97 |
| 6 | 0.541 | 1.18 | 95 | 86 | 85.02 |
| 8 | 0.576 | 1.11 | 97 | 84 | 85.91 |
| 10 | 0.568 | 0.64 | 98 | 85 | 91.88 |

Electrochemical Impedance Spectroscopy (EIS) 0

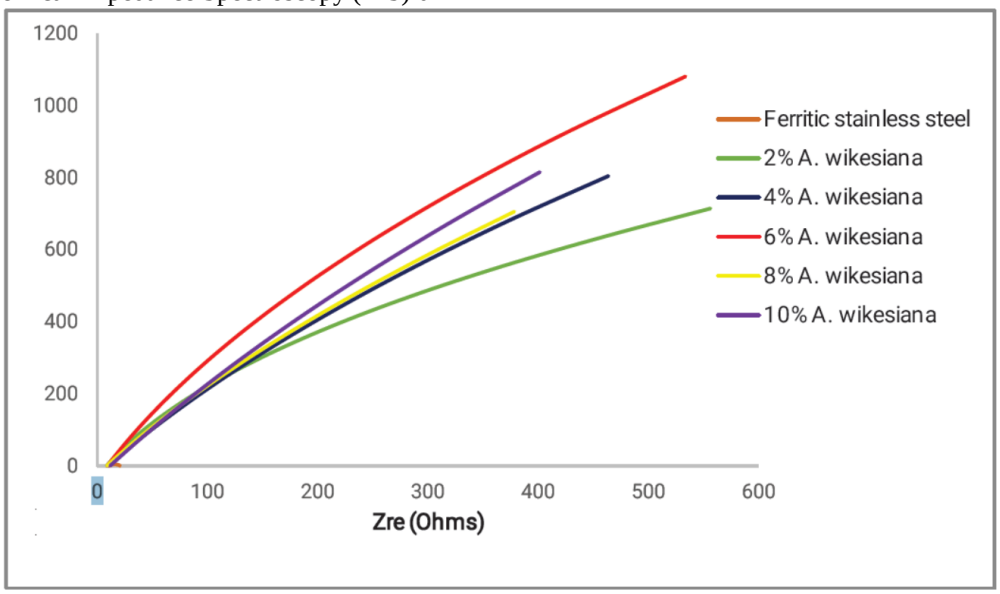


Figure 6: Nyquist plots for Ferritic stainless steel in 1M NaCl in the absence and presence of different concentrations of AW ext

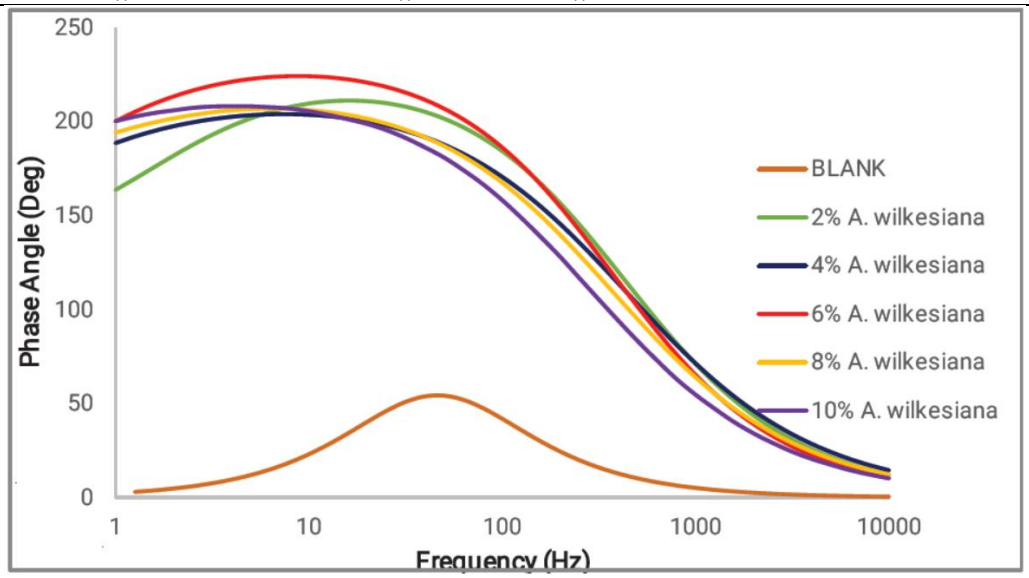


Figure 7: Bode plots for Ferritic stainless steel in 1M NaCl in the absence and presence of different concentrations of AW extract

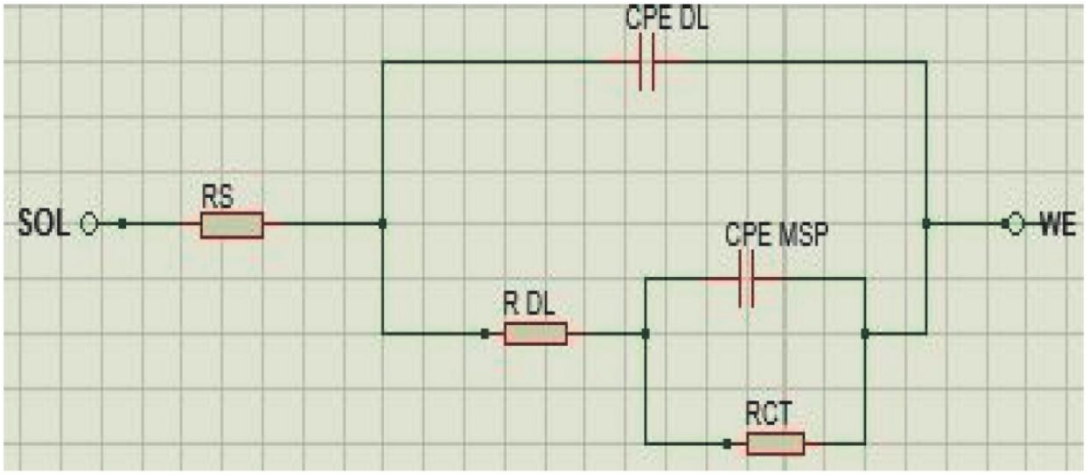


Figure 8: Equivalent circuit for MSP in NaCl

From the Bode plot there was a decrease of the impedence in the capacitive region, the phase angle tends towards zero at low frequencies showing that the resistance of the barrier layer was been approached.

**Gas Chromatography- Mass Spectrometry (GC-MS) analysis of Acalypha wilkesiana extract**

The analysis of Acalypha wilkesianaby GC-MS permitted the classification of fifty mechanism, that comprises of 100% in the total of the extract. Table 9 showed the chemical compounds recognized in the ethanol distillate of Acalypha wilkesiana (AW) leaf extract by GC-MS analysis. The table revealed the presence of 1,3-Benzenediol, 2- chloro, 4-Ethynyl-1- methylpyrazole, 1-ethenyl-1-methyl-2, methyl ester, 2,4- Pentadienenitrile, and other phenolic compounds followed by methyl ester which are major constituents. The results also revealed the functional groups which are good corrosion inhibitors as reported by (Petchiamaletal; 2013 and Suleiman and Sani, 2018,). This extract contains oxygen atoms, hydroxyl, aromatic rings and hydrocarbon which are the centers of adsorption as reported by (Somaz, 2014 and Oguzie 2006).

Table 9: The chemical compounds identified in the ethanol distillate of AW leaf extract by GC-MS analysis

| Peaks | Extract | Chemical Names | Molecular Formula: | Molecular Weight g/mol |
|---|---|---|---|---|
| 1 | | Methane, chloromethoxy- | $C_2H_5ClO$ | 80.523 |
| 2 | | 1,3-Benzenediol, 2 chloro- | $C_6H_3ClN_2O_6$ | 234.5 |
| 3 | | 3-Vinyl-1-cyclobutene | $C_5H_8$ | 80.13 |
| 4 | | 4-Ethynyl-1-methylpyrazole | $C_6H_6N_2$ | 106.128 |
| 5 | | 1-Buten-3-yne | $C_4H_4$ | 52 |
| 6 | ---------- | Difluoroamine | $F_2HN$ | 53 |
| 7 | | 2,4-Pentadienenitrile | $C_5H_5N$ | 79 |
| 8 | | 1,2,4,5,9,10 Triepoxydecane | $C_{10}H_{16}O_3$ | 128 |
| 9 | Acalypha Wilkesiana (AW) | 1-Methyl-3-butenyl 3-methyl-3-hydroxybutyl ether | $C_{10}H_{20}O_2$ | 171.26 |
| 10 | | 10-Azido-1-decanethiol | $C_{10}H_{21}N_3S$ | 215.35 |
| 11 | | 3-Hexen-1-OL | $C_6H_{12}O$ | 100 |
| 12 | | 1-Heptene, 4-methyl- | $C_7H_{14}$ | 98 |
| 13 | | Hexahydro-1,3 benzodioxol-2-one | $C_7H_{10}O_3$ | 142.5 |
| 14 | | Butylamine | $C_4H_{11}N$ | 73.1 |
| 15 | | 1,5-Heptadiene, (Z)- | $C_7H_{12}$ | 96.17 |
| 16 | | 1 azabicyclo(3.1.0)hexane | $C_5H_9N$ | 83.13 |
| 17 | | 5-Nitro-1-pentene | $C_5H_9NO_2$ | 115.13 |
| 18 | | 11-(2-Cyclopenten-1-yl) undecanoic acid, (+) | $C_{16}H_{28}O_2$ | 252.39 |
| 19 | | 11-(2-Cyclopenten-1-yl) undecanoic acid, (+)- | $C_{16}H_{28}O_2$ | 252.39 |
| 20 | | Chlorine dioxide | $C_lO_2$ | 67.45 |
| 21 | | 3-Aminopropionitrile | $C_3H_6N_2$ | 70.09 |
| 22 | | Oxirane, 2,2'-(1,4-butanediyl)bis | $C_8H_{14}O_2$ | 142.19 |
| 23 | | Glycine, N-acetyl- | $C_4H_7NO_3$ | 117.10 |
| 24 | | 3,4-Altrosan | $C_6H_{10}O_5$ | 162.14 |
| 25 | ---------- | (6E)-3-Chloro-6-imino-1(6H)-pyridazinol | $C_4H_4C_lN_3O$ | 145.54 |
| 26 | | 5-(Hydroxymethyl)-1,4-dioxan-2-yl]methanol | $C_6H_{12}O_4$ | 148.15 |
| 27 | | Pentane, 2,2,4-trimethyl- | $C_8H_{18}$ | 114.22 |
| 28 | | D-Mannoheptulose | $C_7H_{14}O$ | 114.23 |
| 29 | | Triepoxydecane | $C_{10}H_{16}O_3$ | 184.23 |
| 30 | | Carbamodithioic acid, dimethyl-, methyl ester | $C_4H_9NS_2$ | 135.25 |
| 31 | | IUDWIAICWHVSQF-UHFFFAOYSA-N | $C_{15}H_{26}O$ | 222.37 |
| 32 | | Nonanoic acid | $C_9H_{18}O_2$ | 158.23 |
| 33 | | Cyclopropanetetradecanoic acid, 2-octyl-, methyl ester | $C_{26}H_{50}O_2$ | 394.67 |
| 34 | | alpha-Methyl-dgalactoside | $C_7H_{14}O_6$ | 194.18 |
| 35 | | Methyl d-glycero-.beta.-dgulo- heptoside | $C_7H_{14}O$ | 114.13 |

| | | | | |
|---|---|---|---|---|
| 36 | | Methyl 6-O-secbutylhexopyranoside | $C_{11}H_{22}O_6$ | 250.29 |
| 37 | | Methylfructoside | $C_7H_{14}O_6$ | 194.18 |
| 38 | | 2,3,4,5,6 Pentahydroxy-7-methoxyheptanal | $C_8H_{16}O$ | 128.12 |
| 39 | | 11-(2-Cyclopenten-1-yl) undecanoic acid, (+)- | $C_{16}H_{28}O_2$ | 252.39 |
| 40 | | Diethylene glycol, 2TMS derivative | $C_{10}H_{26}O_3Si_2$ | 250.48 |
| 41 | ---------- | Methyl d-glycero-.beta.-dgulo- heptoside | $C_7H_{14}O$ | 114.13 |
| 42 | | 11-Cyclopentylundecanoic acid | $C_{16}H_{30}O_2$ | 254.41 |
| 43 | | 7-Octenoic acid | $C_8H_{14}O_2$ | 142.19 |
| 44 | | Cyclopentaneundecanoic acid | $C_{16}H_{30}O_2$ | 254.41 |
| 45 | | Methyl-4,6-O-benzylidene-α-D-galactopyranoside | $C_{14}H_{18}O_6$ | 282.29 |
| 46 | | Lactose | $C_{12}H_{22}O_{11}$ | 342.3 |
| 47 | | 7-Octenoic acid | $C_8H_{14}O_2$ | 142.19 |
| 48 | | Glucose | $C_6H_{12}O_6$ | 180.12 |
| 49 | | 11-Cyclopentylundecanoic acid | $C_{16}H_{30}O_2$ | 254.41 |
| 50 | | 6-Ethyldecan-3-yl prop-2- enoate | $C_{15}H_{28}O_2$ | 240.38 |

**Surface characterization**

The morphology of the examples without and with inhibitor of Acalypha wilkesiana (AW) was inspected and the outcomes exhibited in figure 9a-c. It just uncovered the cleaned/scratched surface. From the surface morphology of uninhibited FSS in 1 M Nacl interface in figure 9b, serious pits, cracks and particular disintegration of inter-metallic happened at the surface. In figure 9c, there was an improvement in the surface morphology of FSS in the nearness of Acalypha wilkesiana (AW). From the SEM assessment, it is clear that a portion of the dynamic constituents in the phytochemical and the FTIR such as CH2, R=CH=CH=R, C=CH2 mono, 1,1, C=C stretch, =N=C=S, C=N, CH2, NH2, X=Y and XY=Z, NH2 act as reaction centre leading to the formation of film on the surface of FSS (Suleiman and Sani, 2017 and Ahmed et.al; 2014). The inhibitor therefore forms a protective thin layers and complexes on the FSS surface. This leading a reduction in contact between.

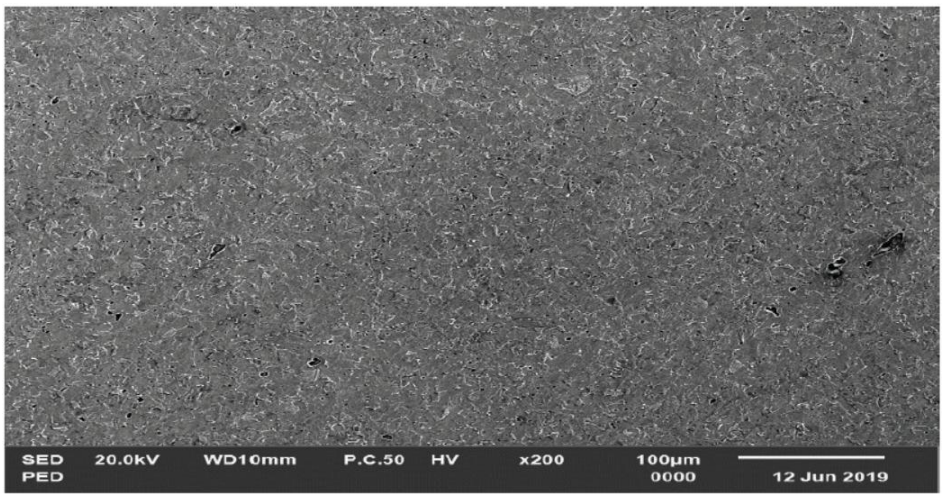


(A)

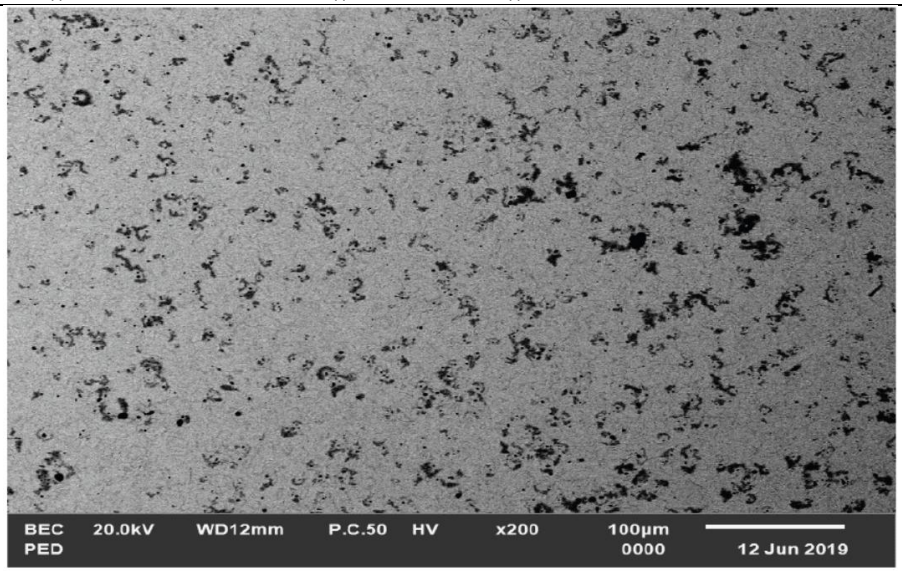


(B)

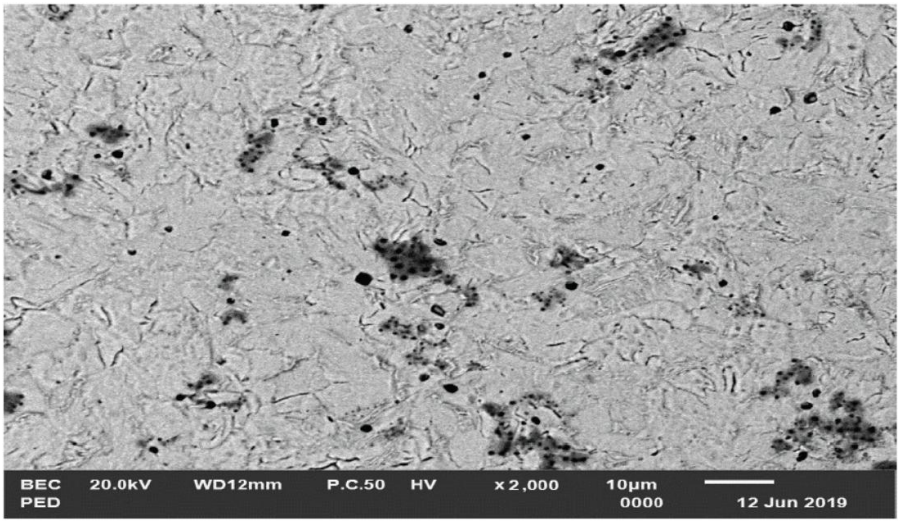


(C)

Figure 9: SEM micrographs of stainless-steelsurface (a) free surface of ferritic stainless steel, (b) after immersion in 1 M Nacl and (c) after immersion in 1 M Nacl + 8% v/v ofAW.

**Adsorption isotherms**

Adsorption isotherm gives the connection between the coverage of an interface with the adsorbed species and the concentration of species in alkaline solutions. The adsorption of various groupings of Acalypha Wilkesiana (AW) extract on the outside of FSS was found to obey Langmuir adsorption isotherm as is in figure 10. The thermodynamic parameters for the adsorption of the concentrate on FSS surface in 1 M Nacl at various temperatures were exhibited in table 10. From the table, it was discovered that the negative estimations of $\Delta G°$ ads reflect that the adsorption was unconstrained procedure and $\Delta G°$ ads values increment (become more positive) with an expansion in temperature. Kads diminishes as the temperature expands which likewise affirm that the green inhibitor was adsorbed and repressed the corrosion. This demonstrated the event of exothermic procedure whereby, adsorption was ominous with expanding response temperature was the aftereffect of the concentrate desorption from the FSS surface (Pereira, 2012).

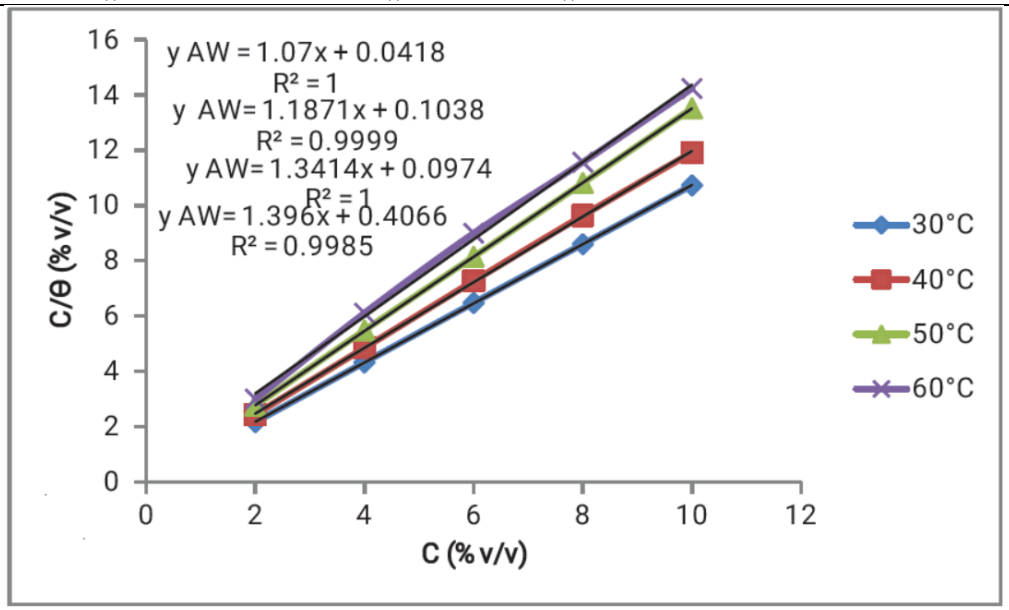


Figure 10: Langmuir isotherm for the adsorption of the AW on stainless steel surface in 1M NaCl solution obtain by gravimetric method at 30, 40, 50, and 60$^{o}$C

Table 10: Parameters from Langmuir Isotherm for AW at 30 - 60$^{o}$C in 1M NaCl solution

| Inhibitor | Temp. | LANGMUIR ISOTHERM | | | |
|---|---|---|---|---|---|
| | ($^{o}$C) | ΔGcorr, KJ/mol | Slope | $R^2$ | $K_{ads}$ |
| | 30 | -12.812 | 1.321 | 0.989 | 1.934 |
| | 40 | -13.453 | 1.134 | 0.996 | 1.497 |
| | 50 | -13.123 | 1.077 | 0.997 | 1.234 |
| | 60 | -13.043 | 1.023 | 0.998 | 1.199 |

Effect of inhibitor concentrations on corrosion rate and inhibition efficiencies The corrosion rates of the samples reduced with immersion time but increased with rise in temperature. From the Figures, the variation of corrosion rates with temperature was in the sequence of 60$^{o}$C >50$^{o}$C>40$^{o}$C >30$^{o}$C. That is, the corrosion rates decrease with increase in green inhibitor and sodium benzoate concentrations at all the temperatures studied. The results further show that as the immersion time increases, the corrosion rate decreases.

**Effect of immersion time on corrosion rate**

Table 7 and Figures 4 show the results of effect of immersion time on stainless steel corrosion inhibition by Acalypha wikesiana extract and control (sodium benzoate inhibitor). From the Table, the results revealed that the extract of Acalypha wikesiana shows the optimum inhibition efficiency of 90.50% at 18 days of immersion time and the inhibition efficiency decreases from 90.50% to 89.20% as immersion time increases from 9 days to 18 days in 1M NaCl. It is evident that the inhibition efficiency increases initially and after attaining optimum concentrations, it decreases with immersion time, resulting to adsorption-desorption processes which also agrees to the findings of Pandian and Mathur, (2010).

**Effect of the temperature**

Temperature has great effect on the corrosion phenomenon and in general, the corrosion rate increases with increase temperature. The effect of temperature on the corrosion rate and inhibition efficiency of ferritic stainless steel (FSS) in 1M NaCl containing optimum concentration 10% (v/v) for Acalypha wikesiana (AW) extract after 18 days from 30-60°C using weight loss measurements were investigated. The results of the effect of temperature on corrosion rate were presented in figures 4 and these also agree with previous studies of (Wang et al., 2006). It is clear that the increase of the corrosion rate is more pronounced with the rise in temperature in the presence of the green inhibitor. Also, the inhibition efficiency decreases slightly with increasing temperature as shown in figures.

Table 11: Activation parameters Ea, ΔHads and ΔSads for FSS dissolution in 1M NaCl in the absence and the presence of AW at 30, 40, 50, and 60°C

| System/concentration | -Ea (kJmol$^{-1}$) | ΔHads kJ/mol | ΔSads(J/mol.k) |
|---|---|---|---|
| Blank | 8.18 | -10.17 | -167.13 |
| 2% v/v AW | 9.08 | -6.87 | -166.11 |
| 4% v/v AW | 9.57 | -8.06 | -160.12 |
| 6% v/v AW | 13.13 | -5.21 | -168.15 |
| 8% v/v AW | 13.73 | -8.77 | -156.05 |
| 10% v/v AW | 15.30 | -9.27 | -154.51 |

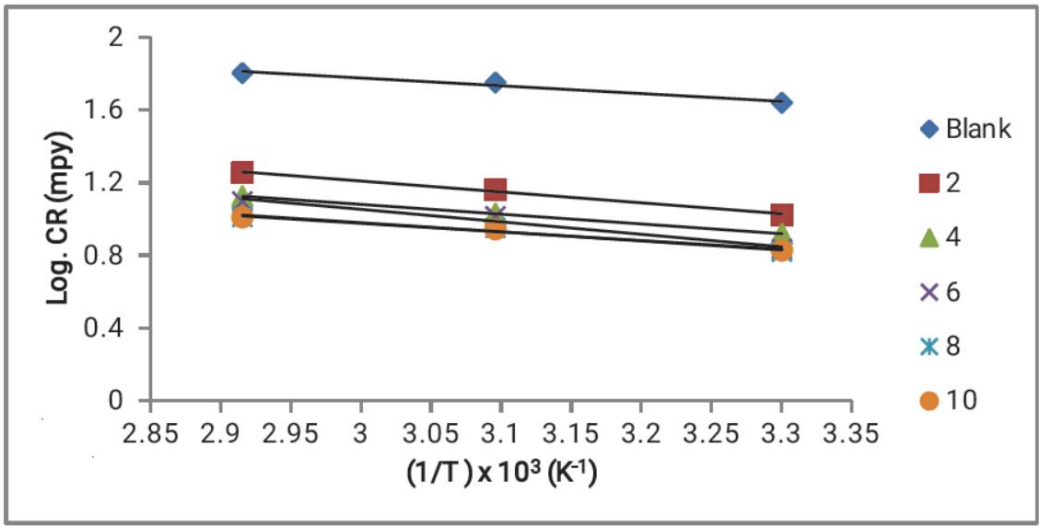


Figure 13: Variation log CR with 1/T for FSS in 1 M Nacl in the presence and absence of AW concentration at 30, 40, 50, and 60°C

The corrosion rate in alkaline solution is associated with Arrhenius equation of temperature provided in equation 5 (Verma et al; 2016 and Xhanai et al; 2016): CR= Aexp (-Ea/RT)5. The plots of log (CR / T) versus 1/T were shown in Figure 13 as a straight row with slope and interval equal to-Hads/2.303R and (log(R / Nh)+Sads/2.303R) respectively from which the values of the slope and intercept had been calculated. Table 11 presented the calculated values for the green AW inhibitor in 1 M Nacl for the activation energy, standard free energy change, Ea, and ambigads for the green AW inhibitor.

## Conclusions

The following conclusions can be drawn from the study investigated:

1. The isothermic adsorption of Langmuir corresponds to the experimental data acquired in this research. Thus, on the ferritic stainless steel surface, a monolayer film was formed by the extract and the values of Ea, Gads, Hads and Sads obtained proposed physical adsorption phenomena for inhibitor adsorption.
2. The adsorbed protective film's SEM morphology on the FSS surface verified elevated performance of the green extract's inhibitive impact.
3. The findings achieved using various analysis of corrosion (gravimetric and potentiodynamic polarization) are inappropriate contracts.
4. The analyses revealed the presence of phytochemical and phytoconstituents in the Acalypha wilkesianasuch as saponins, alkaloids, flavonoids, tannins etc.
5. The results of FT-IR analysis revealed the presence of Thiocarnonyl (C=S), Sulphides compound (SxOy compounds), C-Br Stretching of halogen derivatives etc.
6. The GC-MS also revealed the following structures 1,3-Benzenediol, 2- chloro $C_6H_3C_lN_2O_6$, Ethynyl-1-methylpyrazole $C_6H_6N_2$, Difluoroamine $F_2HN$, 10-Azido-1- decanethiol $C_{10}H_{21}N_3S$, Diethylene glycol, 2TMS derivative $C_{10}H_{26}O_3Si_2$, Carbamodithioic acid $C_4H_9NS_2$, (6E)-3-Chloro-6-imino-1(6H)-pyridazinol $C_4H_4C_lN_3O$ etc.

## References

[1]. Ahamed, H.A.U, Uddin MH, Mannan MA, Barua S, Hoque MA (2014) Studies on the isolation, physico-chemical characterization and microbial activities of melon (Cucumis melon) seed oil.Int J Innov. Sci. Res. 11:105–111 6(4), 1003-1008.

[2]. Adindu, C.B, Oguzie E.E (2017) Investigating the extract constituents and corrosion inhibitingability of Sidaacutaleaves. World News Nat Sci 13:63–81.

[3]. Anupama, KK, Ramya K, Joseph A (2016) Electrochemical and computational aspects of surface interaction and corrosion inhibition of mild steel in hydrochloric acid.

[4]. Dourna, Asefi.,Mokhtar, Arami., Niyaz, Mohammad Mahmoodi. (2011). Organic Materials as Corrosion Inhibitors for Aqueous Medium: A Review. The Electrochemical Society Meeting, 23-56.

[5]. Khadraoui A, Khelifa M, Hadjmeliani R, Mehdaoui K, Hachama A, Tidu Z, Azari IB, Obot A, &Zarrouk, A (2016) Extraction, characterization and anti-corrosion activity of Mentha pulegium oil: weight loss, electrochemical, thermodynamic and surface studies. J Mol L 216:724–731.

[6]. Pandian, Bothi Raja., Rahim, Afidah Abdul., Osman, Hasnah., Awang Khalijah. (2010). Inhibitory Effect of Kopsia Singapurensis Extract on the Corrosion Behavior of Ferritic stainless steel in Acid Media. Acta Phys. Chim. Sin, 26(8), 2171-2176.

[7]. Pereira SSAA (2012) Inhibitory action of aqueous garlic peel extract on the corrosion of carbon steel in HCl solution. Corros Sci 65: 360-366.

[8]. Petchiammal A., Selvaraj S. and K . Kalirajan (2013). Influence of Hibiscus Esculenta Leaves onthe corrosion of Stainless Steel in acidic medium., International Journal of Universal Pharmacy and Bio Science 2(1). 236-246.

[9]. Rajendran A. and Karthikeyan C. (2012). The inhibitive effect of extract of flowers of Cassia Auriculata in 2 M HCl on the corrosion of aluminium and mild steel. Int. J. Plant Res. 2:9-14.

[10]. Rekkab, S. Zarrok, H., Salghi, R., Zarrouk, A., Bazzi, Lh., Hammouti, B., Kabouche, Z, Touzani R, Zougagh M. (2012). Green Corrosion Inhibitor from Essential Oil of Eucalyptus globulus (Myrtaceae) for C38 Steel in Sulfuric Acid Solution", Journal of Materials Environmental Sciences, 3: 613-627.

[11]. Saratha, R., Vasudha, V. G. (2009). Inhibition of Ferritic stainless steel Corrosion in 1N H2SO4 Medium by Acid Extract of Nyctanthes Arbortristis Leaves. E-Journal of Chemistry, 6(4), 1003-1008.

[12]. Suleiman I. Y. and Sani. A. Salihu (2018). Characterizations of Plant Extract by AAS and GC–MS as Green Inhibitor for Mild Steel in 1.0 M HCl. Iran J Sci Technol Trans Sci., 42:1977- 1987.

[13]. Suleiman, Y., Sani, A. S, (2017): Characterizations of Plant Extract by AAS and GC– MS as Green Inhibitor for Mild Steel in 1.0 M HCl. Iranian Journal of Science and Technology, Transactions A: Science, https://doi.org/10.1007/s40995-017-0384- 9

[14]. Suleiman, I. Y., Yaro S. A and Abdulwahab M. (2016).Inhibitive Behaviour of Acacia senegalensis on Corrosion Resistance of Mild Steel-Acidic Environment. Asian Journal of Chemistry; 28(2): 242-248.

[15]. Solmaz, R (2014) Investigation of corrosion inhibition mechanism and stability of Vitamin BI on mild steel in 0.5 M HCl solution. Corros Sci 81:75–84. https://doi.org/10.1016/j.corsci.2013.12.006.

[16]. Suleiman I. Y. and Sani. A. Salihu (2018). Characterizations of Plant Extract by AAS and GC– MS as Green Inhibitor for Mild Steel in 1.0 M HCl. Iran J Sci Technol Trans Sci., 42:1977- 1987.

[17]. Suleiman, I.Y.,Yaro, S. A and Abdulwahab M. (2016).Inhibitive Behaviour of Acacia senegalensis on Corrosion Resistance of Mild Steel-Acidic Environment. Asian Journal of Chemistry; 28(2): 242-248.

[18]. Verma, C.Quraishi M.A, Ebenso, E.E, Obot IB, El Assyry A (2016) 3-Amino alkylated indoles as corrosion inhibitors for mild steel in 1 M HCl: Experimental and theoretical studies. J MolLiq 219:647–660. https://doi.org/10.1016/j.molliq.2016.04.024.

[19]. Xhanari K, Finsˇgar M (2016) Organic corrosion inhibitors for aluminium and its alloys in acid solutions: a review. RSC Adv6:62833–62857.